RSC Advances

Volume 1 | Number 1 | Jan 2013 | Pages 1–100

RSC Advances

www.rsc.org/advances

ROYAL SOCIETY OF CHEMISTRY

ROYAL SOCIETY OF CHEMISTRY

www.rsc.org/advances

RSC Advances

PAPER

Fabrication of complex PDMS microfluidic structures and embedded functional substrates by one-step Injection moulding

C. Szydzik [a], B. Niego [b], G. Dalzell [a], M. Knoerzer [a], F. Ball [a,c], W.S. Nesbitt [a,b], R.L. Medcalf [b], K. Khoshmanesh [a], A. Mitchell [a]

We report a novel injection moulding technique for fabrication of complex multi-layer microfluidic structures, allowing one-step robust integration of functional components with microfluidic channels, and fabrication of elastomeric microfluidic valves. This technique simplifies multi-layer microfluidic device fabrication, while significantly increasing device functionality. We demonstrate functional component integration through robust encapsulation of porous polyester membranes, in the context of an *in-vitro* research platform intended to facilitate Blood Brain Barrier (BBB) research. We also demonstrate the fabrication of normally-closed, pneumatically actuated elastomer valves, integrated using the same one-step process. These valves are demonstrated in the context of variable flow resistors used to modulate flow in a pressure driven system.

Introduction

Microfluidics has flourished in recent years as an emerging technology for addressing a wide range of research applications [1-5]. Perhaps most notably, microfluidics has shown significant promise in revolutionising the biomedical field [6-9]. Hybrid microfluidic devices have been reported incorporating integrated structures such as electrode arrays [10], permeable membranes [11], micro-valves [12, 13] and other functional structures, enabling complex lab-on-a-chip research platforms and point-of-care devices. Numerous microfabrication techniques have been reported for the realisation of microfluidic devices. These commonly use the material polydimethylsiloxane (PDMS) due to its favourable chemical, mechanical, and optical properties, as well as its inherent biocompatibility [4, 14, 15].

Methods for effective and reliable fabrication of complex multi-layer PDMS microfluidic structures incorporating functional structures such as valves, pumps, mixers, membranes and electrodes are crucial for further development of point-of-care and lab-on-a-chip devices. One key challenge is to achieve multiple microfluidic channels on different vertical planes as well as vertical interfaces between those channels without prohibitive fabrication complexity.

Reported fabrication techniques for realising such complex structures can be divided into three primary categories. The first category relies on sequential traditional 2D microfabrication to achieve multi-layer systems [14, 16-19]. This approach has been the mainstay for realisation of complex microfluidics for over a decade, however while the devices have steadily increased in complexity, this fabrication technique has not evolved significantly in the passing years [4, 11, 13, 20, 21]. While layering of 2D microfabricated structures is appealing due to its maturity, complex systems often require multiple manual alignment and bonding processes, which require great skill, making them unsuitable for high volume fabrication.

The second category of fabrication that can achieve multi-layer structures is casting of PDMS around a 3D sacrificial structure, which is later removed or dissolved [22-25]. This approach eliminates the alignment and bonding issues of layered approaches, however these methods often require complex protocols involving removal of the sacrificial structure, which can limit the geometry, impact yield, or again, require skilled manual processing. The third category that has shown particular promise is the mould based 'membrane sandwich' approach, first presented by the Whitesides research group [26]. This fabrication technique simplifies the fabrication of layered channel structures by sandwiching PDMS pre-polymer between a patterned wafer based mould and a passivated PDMS mould. This approach has the advantage of simplifying processing and offers simple mould removal. However, while fabrication techniques have been developed along similar lines [27], there are few reports of complex

a. *School of Electrical and Computer Engineering, RMIT University, Melbourne, VIC 3001, Australia*
b. *Australian Centre for Blood Diseases, Monash University, Melbourne, Australia*
c. *Institute for Optofluidics and Nanophotonics (IONAS), University of Applied Sciences Karlsruhe, 76133 Karlsruhe Germany.*

microfluidic devices realised using this approach, and it would appear that this technique has not been widely adopted and developed by the community.

In this paper, we present an enhanced membrane sandwich based microfluidic fabrication technique, which enables accessible monolithic integration of complex microfluidic structures such as valves, as well as hybrid integration of various functional elements, such as commercial porous membranes used as interfaces between microfluidic channels on different vertical planes. This one step process realises multi-layer microfluidic structures utilising reusable moulds fabricated with high-resolution photolithography as well as rapid and flexible direct 3D printing. We demonstrate the utility of our approach through realisation of an *in-vitro* platform simulating the brain blood barrier, and also pneumatic valves, which can regulate pressurised fluid flow.

Concept

Consider the situation illustrated in **Fig. 1**. If two complementary moulds are placed in contact and PDMS pre-polymer is injected between them, then small voids between the moulds will be filled with PDMS, allowing two independent channels to be formed, which are isolated vertically by a PDMS membrane of controlled thickness. Sufficiently thin membranes could be realised to allow pneumatic distortion in order to achieve valves. If the two moulds are designed to make contact and are pressed together firmly while injecting and curing the PDMS, it should be possible to exclude the PDMS from between the two moulds that are in contact, creating vertical interfaces between the microfluidic channels on different layers, allowing controlled interconnects or isolated overpasses as required. Functional structures could

Fig. 1 Conceptual illustration of PDMS injection moulding fabrication technique. (A) Complementary mould halves are initially loaded with a functional substrate for integration, (B) The moulds are then brought into contact and clamped, (C) Degassed PDMS is injected through an opening and fills voids between the mould structures. The mould assembly is then placed in an oven at 70°C for one hour until cured (D and E) Upon removal of the mould structure the resultant double sided PDMS slab is cut to size, and channels on either side of the slab are sealed with glass slides.

also be embedded within the PDMS block and interfaced to the microfluidic channels from both sides.

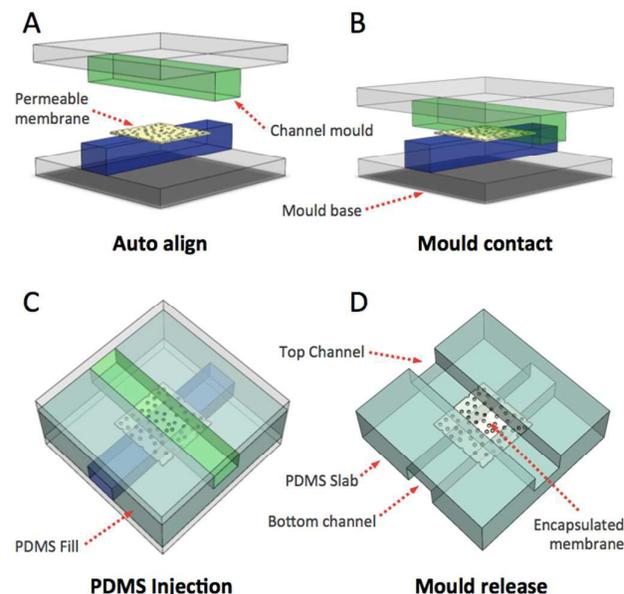**Fig. 1** conceptually illustrates the fabrication technique

Fig. 2 Concept for integration and encapsulation of prefabricated functional components. (A) Transwell permeable support membrane is placed on a point of intersection of the microfluidic mould structures, (B) The complimentary mould structures are then brought into intimate contact and clamped, (C) PDMS is then injected through an opening and fills the voids between moulds, (D) During this process PDMS infiltrates all areas of the membrane not mechanically compressed, resulting in clear areas at the channel intersection and mechanically encapsulated areas without.
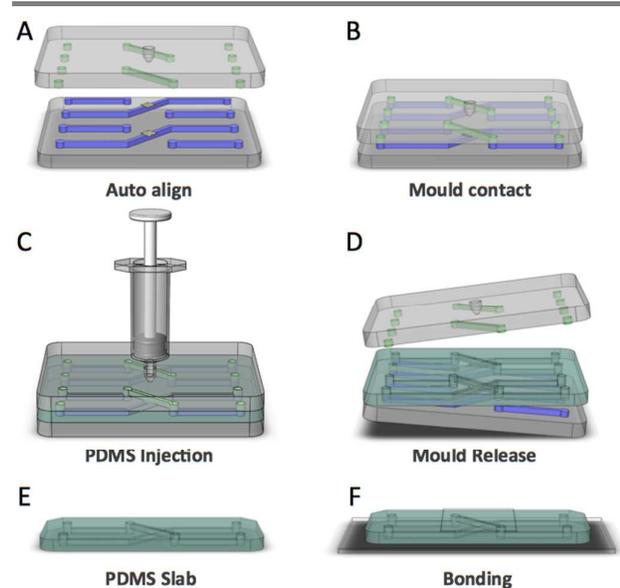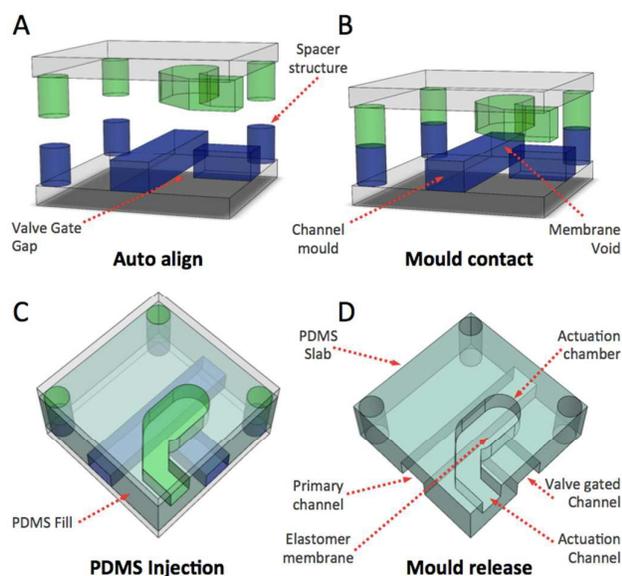
with **Fig. 1 A-F,** illustrating the two mould halves being automatically aligned by peg and hole structures in the mould. The moulds are brought into contact, PDMS is injected to fill voids and create a PDMS slab, followed by mould release and final chip assembly.

Fig. 2 A-D illustrate how prefabricated functional structures can be integrated into microfluidic systems using this fabrication technique. Complementary mould structures are positioned to sandwich an aligned prefabricated functional device, in this case a porous membrane, to achieve a fluidic channel co-culture chip [11]. The complementary mould structures are brought into contact, applying pressure to both sides of the sandwiched device. PDMS is then injected into the mould structure to fill the voids, fully encapsulating the device with the exception of the area excluded by pressure with the raised channel structures within the mould. This approach allows for robust integration of the prefabricated device, interfaced to the microfluidic channels within the PDMS slab.

This fabrication technique can also be applied to realise robust monolithic double-layer functional structures, including pneumatic valves and pumps. **Fig. 3 A-D** illustrate the concept used to fabricate normally-closed, pneumatically actuated valves [28, 29] The complementary mould halves are initially self-aligned and brought into contact. A spacer structure, either directly integrated into the mould or added during moulding depending on the mould fabrication technique used, keeps the

Journal Name

ARTICLE

Fig. 3 Concept for fabrication of active elastomer structures. (A) The mould halves are designed so as to not quite contact at the location of the valve. (B) The mould halves are again brought into contact leaving a narrow void in the region of the valve, (C) PDMS is injected forming a membrane between the two channels, (D) The valve gate can be actuated through application of negative pressure in the actuation chamber.

moulds separated. The top and bottom moulds are thereby defined such that a certain gap is maintained between the top and bottom channels, allowing injected PDMS to fill the void and form a membrane between them.

Mould Fabrication

In this work, moulds have been realised utilising various microfabrication methods. Standard photolithography microfabrication techniques have been used to create wafer-based moulds for high-resolution applications, while larger structures for low-resolution rapid prototyping applications have been fabricated using 3D printing.
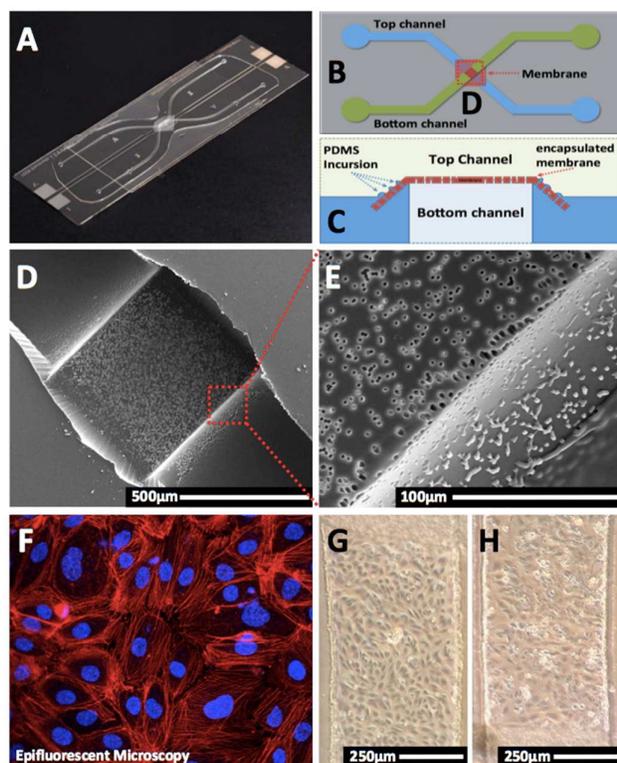
In the case of photolithographically defined moulds, at least one of the mould halves must be optically transparent to allow manual alignment of complementary channels. For this reason, one mould half was patterned onto a 3-inch 2 mm thick borosilicate glass substrate, with the corresponding half patterned on a 4-inch silicon wafer substrate. A borosilicate substrate was used as the top mould as it is optically transparent, allowing for manual alignment. A thickness of 2 mm was used to ensure structural integrity and facilitate the drilling of a 4 mm Luer-connector interface hole for PDMS injection. A 4-inch, 500 µm thick silicon wafer was used as the bottom substrate as silicon has better photoresist adhesion properties than glass. SU-8 3050 series photoresist (MicroChem Corp) was used to produce channel mould structures with a height of 200 µm. The silicon mould half is coated with a 20 nm titanium adhesion layer, followed by a 200 nm gold layer applied using sputter coating. This provides a non-reactive, passivated surface, which facilitates ease of mould release. Upon completion, the two substrates are sandwiched, as outlined in **Fig. 1**. The 4 mm hole in the top

mould half allows coupling with lure type syringe connectors, Highly degassed PDMS is introduced through this opening, and the entire structure is clamped and placed in an oven at 70-80°C to cure. After curing, the two mould halves are carefully opened. The cast PDMS structure begins to separate from the mould spontaneously due to differential thermal contraction of the mould and PDMS, releasing from the passivated mould half first. The slab can then be cut to size and peeled from the unpassivated mould half and the de-moulded PDMS part can then be permanently bonded using oxygen plasma treatment to sealing glass slides. For further information on Injection moulding protocol see **Supplementary S1.** The use of standard photolithographic microfabrication techniques allows for fabrication of high-resolution structures, however the fabrication process is labour-intensive and requires cleanroom facilities.

In contrast, 3D printing can be used to directly print complementary mould structures [25, 30]. This was achieved using a Projet 7000 HD 3D Printer (3DSystems Rock Hill, South Carolina) using the photo curable polymer VisiJet® SL Clear (3DSystems Rock Hill, South Carolina). Structures printed using this material require a post print processing step[25] in order to successfully mould PDMS. This approach allows rapid prototyping when very high-resolution structures are not required, with minimum dimensions defined by the resolution of the 3D printer. In the case of the Projet 7000 3D Printer, 100 µm structures can be fabricated in a reproducible manner. Use of 3D printing, while only applicable for low-resolution structures, greatly simplifies the fabrication process. 3D printing allows for fabrication of vertically tapered structures of varied height [31], such as the otherwise drilled 4 mm Luer-connector interface hole as well as alignment pins and matched wells. These Alignment structures can be fabricated directly into the mould structure, and can be used to self-align the mould structures, eliminating the requirement for manual alignment, and similarly the requirement for optically transparent substrates. Demoulding of the PDMS from the 3D printed moulds was not spontaneous and required manual removal of the PDMS part, this could be due to various factors, such as the different thermal characteristics of the material, as well as lower curing temperature required to avoid mould damage, the absence of a passivated surface, or due to the slightly textured surfaces that result from the 3D printing process. However, manual de-moulding was relatively straightforward due to the larger feature sizes of the 3D print moulded parts.

Results

The technique presented in this paper produces monolithic double-layer PDMS structures, and robust integration of functional structures, fabricated using a one-step process, allowing PDMS to form as a singular slab. Being a single block of PDMS, this monolithic structure is capable of withstanding high pressure and mechanical forces when compared with bonded multi-layer structures. Utility of this technique was verified through realisation of an *in-vitro* microfluidic co-

RSC Advances Accepted Manuscript

ARTICLE

Journal Name

Fig. 4 Shows a Transwell permeable support fully encapsulated in PDMS, in the context of an *in-vitro* model of the blood-brain-barrier. (A) A tissue culture research platform fabricated using the elastomer injection moulding technique. (B and C) Schematic and cross sectional illustration of the membrane area, illustrating the membrane location within the device. (D and E) The point at which the two channels intersect, allowing access to both sides of the permeable support, images obtained using scanning electron microscopy. (F) Representative image of a confocal microscope, demonstrating a monoculture of human endothelial cells cultured within the device; filamentous actin in red, nuclei in blue. (G and H) Phase contrast images of endothelial cells and astrocytes cultured within the micro-channels, as part of a co-culture system.

culture platform with integrated Transwell permeable support cell culture scaffold structures (Corning Inc.) useful for various organ-on-a-chip research platforms [11, 32-35] and also normally-closed pneumatically actuated valves, similar to previous examples from the literature. [28, 29]

Encapsulation of Transwell permeable supports

Application of this technique results in robust integration of Transwell membranes, similar in function to those integrated into other microfluidic systems using standard lamination techniques [36], however embedded in a more robust structure. **Fig. 4** shows a microfluidic research platform fabricated using our novel technique, similar in concept to the *in-vitro* blood brain barrier (BBB) microfluidic model demonstrated by Booth and Kim 2012[36]. We established a contact model of the BBB in our device through co-culture of primary human brain microvascular endothelial cells (ACBRI 376, Cell-Systems Corporation, Kirkland, USA) together with human transformed foetal astrocytes (a cell-line termed SVG [37], Burnet Institute, Melbourne, Australia), on opposite faces of the embedded

membrane. Co-culture was achieved using processes outlined in our previous work [38] adapted for culture within a microfluidic flow based environment, similar to the process outlined in [36]. In brief, endothelial cells are seeded into a fibronectin-treated (Cat. # F1141, Sigma-Aldrich, Australia) channel and allowed to adhere for 2-4 h. The device is then flipped and astrocytes are introduced into the channel interfacing the opposite side of the membrane. Cells are subsequently grown to confluence for 24-48 h under shear stress of 1 dyn/cm^2 prior to experimentation. A detailed culture protocol is specified in **Supplementary S2**. As a major improvement to similar flow devices [36] or to static BBB models [38, 39], our platform is designed to allow high-resolution microscopic access to both sides of the integrated membrane, enabling real-time monitoring of either cell type within the co-culture; since the chip is symmetrical and horizontally opposed, a simple rotation over a microscope objective becomes possible.

Fig. 4 shows a 3 μm pore Transwell permeable support integrated with microfluidic channels and encapsulated within PMDS. **Fig. 4C** illustrates a cross section of the membrane area; the flat area has been compressed by contact between the two moulds, while areas of membrane not compressed during moulding extend into the PDMS slab and are fully encapsulated. Scanning electron microscope images**, Fig. 4D** and **E** further demonstrate how the channels cross at this intersection point with the membrane, forming a permeable barrier between channels. PDMS pre-polymer fluid has a low surface tension and can easily infiltrate very thin gaps. This assists the encapsulation process by fully infiltrating the individual pore structures of the Transwell support in areas of the membrane that are not pressed against the mould during injection moulding, as seen in the lower right of **Fig. 4E.** This process however does not occur in areas of the membrane which are pressed against the mould structures, as can be seen in the flat region on the top left of **Fig. 4E,** demonstrating that with this technique, it is possible to choose where the PDMS will infiltrate and where it will be excluded. Gas bubbles trapped at feature edges or small void features (such as membrane pores) can be avoided by degassing PDMS pre-polymer under high vacuum conditions prior to injection. Once thoroughly degassed, the pre-polymer is able to absorb small bubbles prior to cure, resulting in defect free casting.

Finally, as shown in **Fig. 4F-H**, our channels are fully compatible with cell growth and micro-imaging. Fluorescence confocal microscopy (**Fig. 4F**; Nikon A1r+ confocal microscope) demonstrates actin filaments and nuclei of endothelial cells cultured on the porous membrane embedded within our device. Furthermore, as shown by phase contrast microscopy (**Fig. 4H**), both endothelial cells and astrocytes reach confluence within the micro-channels and cover the entire channel and membrane areas. Hence, our model is well-suited for biological experiments not only in the context of the BBB, but also for numerous other applications. Additional details regarding cell culture protocols are included in **Supplementary S2**.

Journal Name

ARTICLE

Normally closed pneumatically-actuated elastomer valves

Application of this technique results in robust elastomer double-layer structures, and as a proof-of-concept was applied in the context of normally closed pneumatically actuated elastomer valves, similar in principle, to previous reports [28, 29], however, with an inherently more robust monolithic structure, and significantly simplified fabrication process.

As with many normally-closed elastomer valve approaches, undesirable irreversible bonding of the valve gate to the channel sealing substrate can occur. During proof-of-concept experiments, this bonding was avoided by selective PDMS passivation using manual application of ink to the valve gate followed by post bonding ethanol wash out [40]. To avoid this bonding on a larger scale, and with increased reproducibility, various other solutions such as valve actuation prior to bonding [28], or selective surface de-activation [41] can be applied, while the problem can also be avoided using reversible pressure bonding with a clamp structure.

Fig. 5 illustrates validation of these valves, **Fig. 5A** shows an assembled chip, while the cross section in **5B** conceptually demonstrates operation of these valves. Pressurising the actuation chamber relative to the valve gate will close the valve; while evacuating the actuation chamber opens the valve. Applying an intermediate pressure can result in a
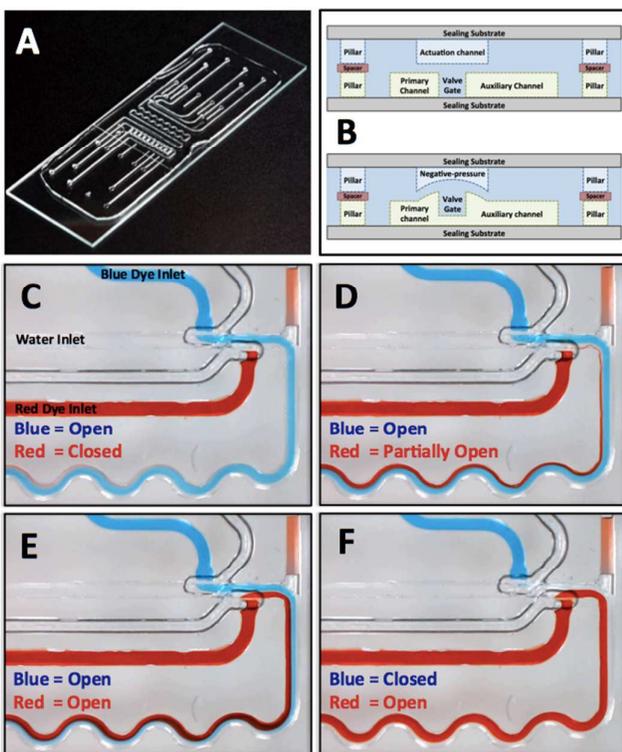

Fig. 5 Pneumatically actuated, normally-closed elastomer valves fabricated using PDMS injection moulding with direct 3D printed mould structures. (A) Shows a proof-of-concept prototype microfluidic system used to demonstrate valve functionality, (B) Shows a conceptual illustration outlining the functional principal of the valves, (C-F) Demonstrate operation of these valves as fluidic resistors. Water is introduced at the primary inlet using a syringe pump, and the dyed inlets are fed by reservoirs maintained at slightly positive pressure. Valve actuation chambers are manually pressurised using a syringe to produce full or partial opening of blue and red dye gates.
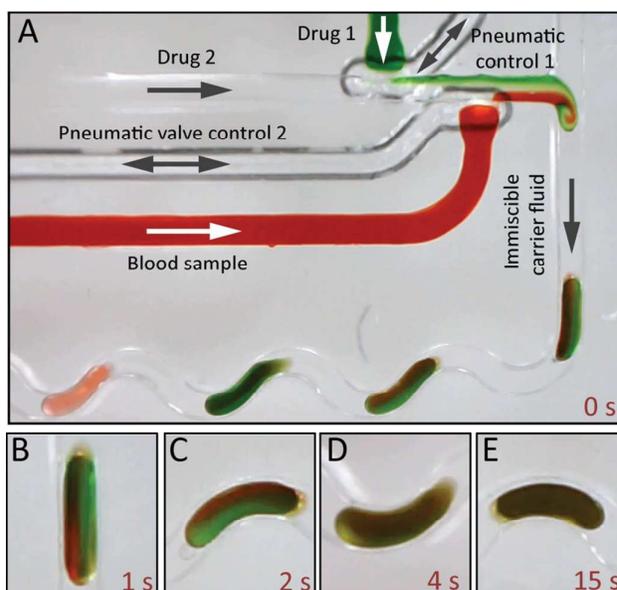

Fig. 6 (A) Application of the pneumatically actuated on chip valves in use as flow regulators of pressure driven fluids in a droplet slug based system. This system is an initial proof-of-concept prototype utilising these valves to actively modulate the component of coloured water dispensed into each droplet, and is planned for investigating the effects of various drug concentrations and combinations on the morphology of blood cells under flow, (B-E) Show mixing of reagents within a slug at various time points.

partially open valve with finite fluidic resistance. In this proof-of-concept demonstration, this pressurisation and evacuation is achieved manually using a syringe[42]. **Fig. 5C-F** qualitatively illustrate the valves in use as variable flow resistors, controlling the confluent flow of water, and coloured water with food dye. (Further detail provided in **Supplementary S3** and **Supplementary Video 1**).

Fig. 6 illustrates valves fabricated using this method modulating the concentration of reagents added to fluid slugs to allow rapid microfluidic mixing. In this arrangement, valves can be used to apply known ratios of fluid to the droplet stream, or fully isolate the dye channel, as would be required in research platforms investigating the effects of known volumes of drug to blood droplets. **Fig. 6A** shows the system configured as in **Fig. 5**, however with the addition of an immiscible fluid flow from the top channel, operation of the system is demonstrated in **Supplementary Video 1**.

Discussion

Most reported fabrication techniques for encapsulation of functional substrates within PDMS, or fabrication of elastomer valves, involve the stacking and bonding of multiple layers of PDMS thin films patterned with channel structures. Valves are commonly fabricated using this method [28], and thin structures can be integrated by lamination between these PDMS films, so long as they are thin enough to allow sufficient adhesion of PDMS layers [32]. While these approaches are well established, they are time-consuming, labour-intensive and error-prone, as all layers must be fabricated, aligned and bonded individually.

These techniques can also lead to platforms that are prone to failure due to leakage caused by various defects, which can occur under different circumstances, including when the layers are not correctly aligned and wrinkles form, when debris is caught in between the two layers, when a pressure differential between the closed channel and ambient environment is significant enough to delaminate the PDMS layers, or a combination of these factors [43].

While bonded multi-layer integration of devices within PDMS is limited to devices thin enough to allow for mechanical deformation of the PDMS to form a seal around the edges, this technique fully encapsulates all surfaces of the device not within the deliberate exclusion zones of the mould, and for this reason is not limited to integration of thin devices. Comparing the practicality of 3D printed and photolithographic moulds: Fabrication using 3D printing allows rapid and arbitrarily reconfigurable prototyping and automatic mechanical mould alignment, however resolution and surface smoothness is limited by the printer used, various materials used in stereolithography require post-print processing steps and mould release is more challenging with these materials. Photolithographically defined moulds allow significantly higher resolution, however require cleanroom fabrication facilities, and make multi-layer moulds cumbersome, limiting the options for automatic mechanical alignment and thereby requiring transparent substrates.

Another consideration is the ease with which the PDMS structure can be de-moulded. In our experiments de-moulding of photolithographically defined moulds begins spontaneously, driven by thermal contraction, whereas the 3D printed moulds required manual removal of the part, however this was relatively straightforward. It is anticipated that design of the mould, cooling protocol and selective surface treatments could be optimised to enhance and control the thermal contraction de-moulding process. It may also be possible to inject gas into the mould to make the cooling and de-moulding even more rapid for scaling to automatic and rapid throughput for both photolithographic and 3D printed moulds. These investigations will be pursued in future work.

Conclusions

We have shown a practical method for the fabrication of monolithic microfluidic devices with complex 3D structures. This method allows for the integration of devices that enable complex functionality for microfluidic systems. This method is also suited to rapid prototyping and reduces fabrication error compared to established methods, allowing for more reliable and complex microfluidic chips to be realised in a short time. This technique allows for reduction in fabrication complexity, while allowing for increase in functional complexity, and could be applied to significantly simplify the fabrication of complex valve based research platforms such as those seen in large scale integration approaches [12, 44]. Future research will investigate hybrid integration of various modular components such as membranes, electrodes, piezo-actuators, heaters, pressure sensors and biosensors within lab-on-a-chip

platforms, with the potential of retaining high-resolution optical access. This technique can also take advantage of the emergence of high resolution 3D printing, enabling reusable moulds for very complex systems incorporating both valve membranes and hybrid integrated elements to be realised rapidly and reliably and should thus mark a major acceleration in the application of microfluidic platforms.

Acknowledgements

References

1. P. N. Nge, C. I. Rogers and A. T. Woolley, *Chemical reviews*, 2013, 113, 2550-2583.
2. K. S. Elvira, X. C. i Solvas and R. C. R. Wootton, *Nature chemistry*, 2013, 5, 905-915.
3. P. M. Valencia, O. C. Farokhzad, R. Karnik and R. Langer, *Nature nanotechnology*, 2012, 7, 623-629.
4. K. Ren, J. Zhou and H. Wu, *Accounts of chemical research*, 2013, 46, 2396-2406.
5. J. Kim, E. C. Jensen, A. M. Stockton and R. A. Mathies, *Analytical chemistry*, 2013, 85, 7682-7688.
6. E. K. Sackmann, A. L. Fulton and D. J. Beebe, *Nature*, 2014, 507, 181-189.
7. B. Xiong, K. Ren, Y. Shu, Y. Chen, B. Shen and H. Wu, *Advanced Materials*, 2014, 26, 5525-5532.
8. E. W. Esch, A. Bahinski and D. Huh, *Nature reviews Drug discovery*, 2015, 14, 248-260.
9. N. Gupta, J. R. Liu, B. Patel, D. Solomon, B. Vaidya and V. Gupta, *Bioengineering & Translational Medicine*, 2016.
10. T. A. Nguyen, T.-I. Yin, D. Reyes and G. A. Urban, *Analytical chemistry*, 2013, 85, 11068-11076.
11. M. W. van der Helm, A. D. van der Meer, J. C. Eijkel, A. van den Berg and L. I. Segerink, *Tissue barriers*, 2016, 4, e1142493.
12. I. E. Araci and P. Brisk, *Current Opinion in Biotechnology*, 2014, 25, 60-68.
13. A. K. Au, H. Lai, B. R. Utela and A. Folch, *Micromachines*, 2011, 2, 179-220.
14. J. C. McDonald and G. M. Whitesides, *Accounts of chemical research*, 2002, 35, 491-499.
15. S. Halldorsson, E. Lucumi, R. Gómez-Sjöberg and R. M. Fleming, *Biosensors and Bioelectronics*, 2015, 63, 218-231.
16. M. A. Unger, H.-P. Chou, T. Thorsen, A. Scherer and S. R. Quake, *Science*, 2000, 288, 113-116.
17. B.-H. Jo, L. M. Van Lerberghe, K. M. Motsegood and D. J. Beebe, *Journal of Microelectromechanical Systems*, 2000, 9, 76-81.

ARTICLE

RSC Advances Accepted Manuscript

18. J. C. Love, J. R. Anderson and G. M. Whitesides, *Mrs Bulletin*, 2001, 26, 523-528.
19. A. D. Stroock and G. M. Whitesides, *Electrophoresis*, 2002, 23, 3461-3473.
20. M. Zhang, J. Wu, L. Wang, K. Xiao and W. Wen, *Lab on a Chip*, 2010, 10, 1199-1203.
21. J. Kim, A. M. Stockton, E. C. Jensen and R. A. Mathies, *Lab on a Chip*, 2016, 16, 812-819.
22. Y. Hwang, O. H. Paydar and R. N. Candler, *Sensors and Actuators A: Physical*, 2015, 226, 137-142.
23. Y. He, J. Qiu, J. Fu, J. Zhang, Y. Ren and A. Liu, *Microfluidics and Nanofluidics*, 2015, 19, 447-456.
24. V. Saggiomo and A. H. Velders, *Advanced Science*, 2015, 2.
25. H. N. Chan, Y. Chen, Y. Shu, Y. Chen, Q. Tian and H. Wu, *Microfluidics and Nanofluidics*, 2015, 19, 9-18.
26. J. R. Anderson, D. T. Chiu, R. J. Jackman, O. Cherniavskaya, J. C. McDonald, H. Wu, S. H. Whitesides and G. M. Whitesides, *Analytical chemistry*, 2000, 72, 3158-3164.
27. J. Hansson, M. Hillmering, T. Haraldsson and W. van der Wijngaart, *Lab on a Chip*, 2016, 16, 1439-1446.
28. R. Mohan, B. R. Schudel, A. V. Desai, J. D. Yearsley, C. A. Apblett and P. J. A. Kenis, *Sensors and Actuators B: Chemical*, 2011, 160, 1216-1223.
29. J. Kim, M. Kang, E. C. Jensen and R. A. Mathies, *Analytical chemistry*, 2012, 84, 2067-2071.
30. G. Comina, A. Suska and D. Filippini, *Lab on a Chip*, 2014, 14, 424-430.
31. S. Waheed, J. M. Cabot, N. P. Macdonald, T. Lewis, R. M. Guijt, B. Paull and M. C. Breadmore, *Lab on a Chip*, 2016, 16, 1993-2013.
32. A. Wolff, M. Antfolk, B. Brodin and M. Tenje, *Journal of pharmaceutical sciences*, 2015, 104, 2727-2746.
33. J. D. Caplin, N. G. Granados, M. R. James, R. Montazami and N. Hashemi, *Advanced healthcare materials*, 2015, 4, 1426-1450.
34. J. S. Lee, R. Romero, Y. M. Han, H. C. Kim, C. J. Kim, J.-S. Hong and D. Huh, *The Journal of Maternal-Fetal & Neonatal Medicine*, 2016, 29, 1046-1054.
35. J. Ribas, H. Sadeghi, A. Manbachi, J. Leijten, K. Brinegar, Y. S. Zhang, L. Ferreira and A. Khademhosseini, *Applied in vitro toxicology*, 2016.
36. R. Booth and H. Kim, *Lab on a chip*, 2012, 12, 1784-1792.
37. E. O. Major, A. E. Miller, P. Mourrain, R. G. Traub, E. De Widt and J. Sever, *Proceedings of the National Academy of Sciences*, 1985, 82, 1257-1261.
38. B. Niego and R. L. Medcalf, *JoVE (Journal of Visualized Experiments)*, 2013, e50934-e50934.
39. B. Niego, R. Freeman, T. B. Puschmann, A. M. Turnley and R. L. Medcalf, *Blood*, 2012, 119, 4752-4761.
40. J. Y. Baek, J. Y. Park, J. I. Ju, T. S. Lee and S. H. Lee, *Journal of Micromechanics and Microengineering*, 2005, 15, 1015.
41. S. CaiáLesher-Perez, *Lab on a Chip*, 2011, 11, 738-742.
42. D. Irimia and M. Toner, *Lab on a Chip*, 2006, 6, 345-352.
43. I. E. Araci, P. Pop and K. Chakrabarty, 2015.
44. P. Pop, W. H. Minhass and J. Madsen, *Microfluidic Very Large Scale Integration (VLSI)*, Springer, 2016.